

# Role of athermal fluctuations in shear flows.

Yuhong Wang, Kapilanjan Krishan, and Michael Dennin

*Department of Physics and Astronomy, University of California at Irvine, Irvine, California 92697-4575*

(Dated: May 25, 2019)

We report on experiments that use velocity measurements as a probe of the underlying fluctuations in sheared two-dimensional foam. We compare time averages and ensemble averages of the velocity profile and quantify a difference between these averages. We discuss the applicability of the ergodic hypothesis and measures of effective temperatures in such systems. We find that the short time athermal fluctuations are not correlated and that the long time velocity profiles retain memory of the initial configurations.

PACS numbers: 05.20.Gg,05.70.Ln,83.80.Iz

A central tenant of statistical mechanics is the ergodic hypothesis: thermodynamic systems pass through almost all possible microstates leading to the equivalence of time and ensemble averages [1, 2, 3, 4, 5]. This is a fundamental characteristic of thermal fluctuations. A pertinent question is whether or not athermal fluctuations lead to the equivalence of time and ensemble averages, especially in complex fluids and mesoscopic systems (e.g. granular matter, foams, colloids, etc.). This is essential to a rigorous understanding of two current areas of research in complex fluids: proposals for effective temperatures [6, 7, 8] and the proposed jamming paradigm [9]. The notion of an effective temperature is based on the assumption that athermal fluctuations induced in driven complex fluids may be characterized in a useful way similar to temperature in systems at thermal equilibrium. A number of definitions of effective temperatures have been proposed [10]; however, quantitative agreement amongst them remains elusive [11]. The jamming transition can occur when fluctuations at a given “temperature” are insufficient to effectively explore phase space to induce flow. The jamming transition has been measured experimentally for certain colloid systems [12]. Simulations support the existence of a special point (the J-point) in the jamming phase diagram that has features of a phase transition [13]. However, it is still an open question as to the connection between the jamming transition and “true” thermodynamic phase transitions, in part due to a lack of a ubiquitous definition of “temperature” in such systems. Also at issue is the role played by fluctuations in the jamming transition and any distinctions between thermal and athermal fluctuations in this context.

The importance of understanding athermal fluctuations stems from the fact that they are ubiquitous in flowing complex fluids. In complex fluids, athermal fluctuations arise through nonlinear particle rearrangements that are induced by flow. As mentioned, the potential for these athermal fluctuations to play a role that is similar to thermal fluctuations in normal fluids is the basis of many statistical treatments of highly non-equilibrium complex fluids. In this paper, we focus on the ability of athermal fluctuations to span phase space produc-

ing equivalent time and ensemble averages. When such equivalence exists, one can use well developed statistical techniques for extracting average properties of the fluid. The average velocity profile is an example of such a property. Its convergence through time and ensemble averages probes their congruity.

Studies of the connection between the average velocity profile and athermal fluctuations address another interesting phenomenon that is observed in complex fluids: shear localization [14, 15, 16, 17, 18, 19, 20, 21, 22, 23, 24]. Shear localization in complex fluids refers to the coexistence of flowing and stationary regions in the material, and is often observed as nonlinear velocity profiles. Shear localization has been observed both experimentally [14, 15, 16, 17, 18, 19] and in simulations [20, 21, 22, 23, 24]. Simulations have pointed to issues of long time-convergence of velocity profiles and comparisons between different studies are often complicated by details of geometry. In this regard, a better understanding of both the long-time and ensemble average process in foams would help resolve some of the open questions.

Finally, in considering any comparison of time and ensemble averages, it is important to recognize that the nature of athermal fluctuations can impact the existence of long time averages. This is highlighted by work in granular matter in which extremely long times were required for convergence of the average density under tapping [25]. This shows that these systems can spend a long time in metastable states, and that the measurement of time-average quantities can be extremely difficult.

In this Letter, we report on measurements of the average velocity profile using a model two-dimensional foam: a bubble raft [26]. One advantage of using a foam is that thermal fluctuations are essentially irrelevant. Aqueous foam consists of bubbles of gas separated by liquid walls. Under an applied constant rate of strain, the initial response of the foam is for the bubbles to stretch elastically. Eventually, bubbles undergo neighbor switching events, referred to as T1 events, that enable flow. These T1 events, and the associated bubble rearrangements, result in fluctuations in the stress, energy, and bubble positions [27]. The interesting feature is that despite the highly

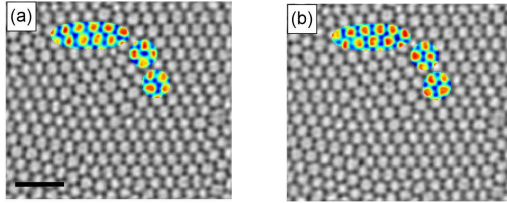


FIG. 1: (color online) Two typical consecutive images representing the instantaneous structure of the bubble raft. Shear induced through the bands on the top and bottom cause the material to yield through slip between neighboring bubbles (T1 events). These local events (bubbles filled in and highlighted in color) cause fluctuations in the velocity profiles of the bubbles, that average out over long times. (The scale bar in image (a) is 1 cm.)

nonlinear and irregular nature of individual T1 events, the long time average of the bubble velocities is usually well defined. The average velocity profile for foam has been the subject of substantial theoretical [22, 23, 28, 29] and experimental [17, 19, 30, 31, 32, 33] work. However, the connection between time and ensemble averages for velocity profiles in foam (and other complex fluids) remains an open question.

In addition to single T1 events, there are collective motions involving many T1 events with large regions of bubble rearrangement. These large scale events can be related to sudden changes of the macroscopic stress stored in the system [34]. As a result of these collective motions, topological variations associated with individual T1 events are transported through the system. These fundamental bubble motions are illustrated in Fig. 1. By generating fluctuations in the velocity due to rapid changes in the positions of the bubbles, these nonlinear transitions may lead to ergodic dynamics when the system is subjected to continual strain.

The bubble raft is produced by flowing regulated nitrogen gas through a needle into a homogeneous solution of 80% by volume deionized water, 15% by volume glycerine, and 5% by volume Miracle Bubbles (from Imperial Toy Corporation). The bubbles are confined between two parallel bands separated by a distance  $d$ . The bands are driven at a constant velocity  $v_w$  in opposing directions. This applies a steady rate of strain to the system given by  $\dot{\gamma} = 2v_b/d$ . The total applied strain is  $\gamma = \dot{\gamma}t$ , where  $t$  is the time interval under consideration. The direction of flow imposed by the bands is taken to be parallel to the x-axis. By tracking the individual motions of the bubbles, we compute the average velocity profile  $\langle v_x(y) \rangle_\gamma$ , where the y direction is taken perpendicular to the bands and  $\langle \rangle_\gamma$  indicates that the average is over a particular strain interval. (Because the experiments are at a constant rate of strain, averages over time and strain differ by only a scalar constant of proportionality.) Here  $v_x(y)$

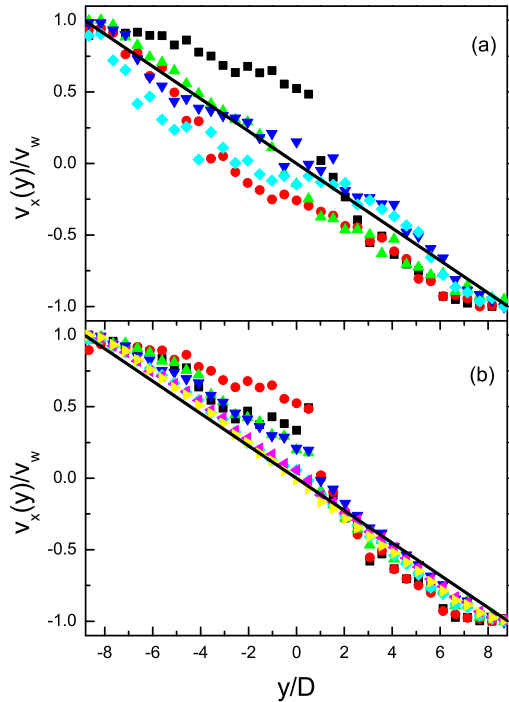


FIG. 2: (color online) The different curves in the upper figure are velocities of the bubbles as a function of the position across the trough. They are each computed over a strain interval of 0.1 taken at different times in the total run. The large fluctuations are induced due to local reorganization of the foam through T1 events. These fluctuations are indicative of the inherent non-Newtonian behaviour of the material. The lower figure indicates the convergence of the velocity profiles through averaging over increasing amount of time (or strain). The symbols (colours) represent increasing intervals of strain in the following order:  $\square$  (black),  $\circ$  (red),  $\triangle$  (green),  $\nabla$  (blue),  $\diamond$  (light blue),  $\triangleleft$  (purple),  $\triangleright$  (yellow).

represents an average over all bubbles in a bin of width  $dy$  at a distance  $y$  from the center between the bands and extended along the x-axis. Unless stated, plots are of the normalized x-component of the velocity ( $v_x/v_w$ ) as a function of the position normalized by the bubble diameter ( $y/D$ ). Details of the apparatus and methods can be found in Ref. [35].

Before comparing time and ensemble averages, it is necessary to establish the convergence of time averages, consistent with a stationary distribution of states during evolution. In addition, the convergence of the time averages provides its own probe of the nature of the athermal fluctuations. Figure 2a illustrates typical velocity profiles that are achieved by averaging over a strain interval of 0.1 taken at different points in a run to total strain 5. A straight line is included as a guide to the eye. This demonstrates the fluctuating nature of short time

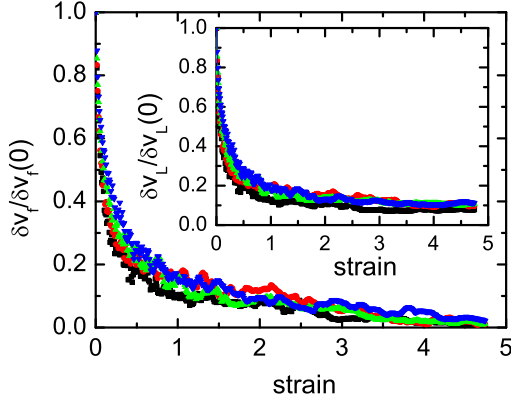


FIG. 3: (color online) The measure of the convergence of the velocity profiles relative to the final average profile ( $\delta v_f(\gamma)/\delta v_f(0)$ ) versus strain for different rates of strain ( $0.0028\text{ s}^{-1}$  ■ (black),  $0.011\text{ s}^{-1}$  • (red),  $0.042\text{ s}^{-1}$  ▲ (green), and  $0.14\text{ s}^{-1}$  ▼ (blue)). The convergence factors have been scaled by the value at a strain of zero for direct comparison between different rates of strain. For comparison, the insert is a plot of the convergence with respect to a linear profile ( $\delta v_L(\gamma)/\delta v_L(0)$ ) for the same experimental runs. The main difference between the two measures is the offset that exists for  $\delta v_L(\gamma)/\delta v_L(0)$ .

velocity profiles. By considering the behavior at different times in the run, we establish the persistence of the fluctuations throughout the entire time during which the flow is imposed on the system. A striking feature of the profiles is the fact that they do not reflect the symmetry of the applied rate of strain. For any given strain interval, we observe profiles that fluctuate above and below the expected straight line behavior, as well as ones that are either consistently above or consistently below this line. As one increases the strain interval used to compute the averages, the average velocity approaches a linear profile more closely, as indicated in Fig. 2b.

To quantify the convergence and the rate of convergence, we measured two different quantities:  $\delta v_L(\gamma)$  and  $\delta v_f(\gamma)$ . Essentially,  $\delta v_L(\gamma)$  measures the deviation of a short-time average from a linear profile and  $\delta v_f(\gamma)$  measures the deviation of a short-time average from the average over the total strain of 5. More specifically,  $\delta v_L(\gamma) = \sqrt{\langle (v - \bar{v}_L)^2 \rangle_\gamma}$  and  $\delta v_f(\gamma) = \sqrt{\langle (v - \bar{v}_f)^2 \rangle_\gamma}$ , where  $v$  is the instantaneous x-component of the velocity,  $\bar{v}_L$  or  $\bar{v}_f$  denotes a linear velocity profile or the average of instantaneous velocities over the total strain applied, respectively. The braces,  $\langle \rangle_\gamma$ , refer to an average over all bubbles being considered, and over a strain  $\gamma$ . Figure 3 indicates the value of  $\delta v_f(\gamma)$  as a function of the total external strain applied to the bubble raft, and the insert in Fig. 3 is a plot of  $\delta v_L(\gamma)$ . The different curves are for different rates of strain. The fact that they essentially

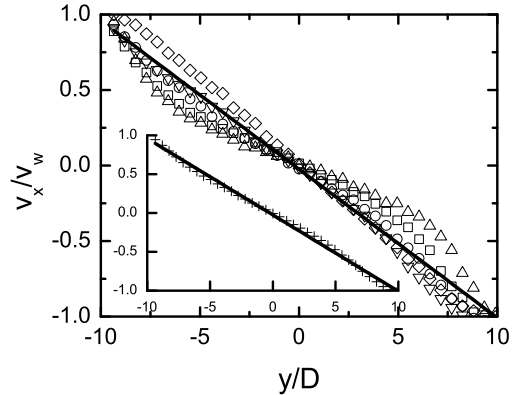


FIG. 4: Velocity profiles for five different realizations of a bubble raft (open symbols) as a function of the position perpendicular to the walls (error in the velocity measurement is equal to or smaller than the symbol size). Straight line represents the expected linear profile for a Newtonian fluid. For comparison, the insert shows the ensemble average of ten runs (crosses) and the same linear profile used in the main figure (solid line).

collapse reflects the independence of the behavior on the rate of strain. The most striking features are that (a) the profiles converge in a well-defined manner and (b) there is a measurable difference between the final velocity profile and a linear profile.

These last two statements relate to the functional form of  $\delta v_L(\gamma)$  and  $\delta v_f(\gamma)$ . Both sets of data are well fit by a double exponential. The difference being that  $\delta v_f(\gamma)$  is well fit with zero offset, establishing that the system is converging to a well-defined final state. However, fits of  $\delta v_L(\gamma)$  consistently require a non-zero offset (on the order of 0.1 for all rates of strain), indicating a measurable difference between the final converged state and a linear profile. The fit to a double exponential suggests that at least two dominant strain scales govern the convergence to the final profile. It is not possible to obtain a good fit with a single exponential. Referring back to the qualitative behavior indicated in Fig. 1, one can associate the shorter strain scale with the individual T1 events and the longer scale with the large collective motions. Further work will be needed to make this statement precise.

Given that the time averages are well-defined, we can compare them with an ensemble average. The primary distinction between the different members of the ensemble are in the initial spatial distributions of the bubbles. A true ensemble average would average over all allowed microstates. To approximate an ensemble average, we average the time-averaged velocity profiles for a series of different initial conditions. As each initial state results in different time-averages, these represent different explo-

rations of the allowed microstates. Therefore, averaging over results for different initial conditions approximates an ensemble average. Because we have already shown that all of the behavior is independent of rate of strain, we will focus on ten different realizations of a bubble raft and determine the velocity profile for each realization using an applied rate of strain of  $0.014 \text{ s}^{-1}$ . Figure 4 is a plot of the 5 different velocity profiles taken from a series of 10 runs and the average of the 10 runs. Each profile represents a strain-averaged profile over a strain of 5. As expected, the differences between the individual profiles are on the same order as their differences from a linear profile (as measured by  $\delta v$ ). Therefore, each realization of the bubble raft results in a different time-averaged velocity profile. Comparing the averaged profile for the 10 runs and a linear profile gives  $\delta v_L = 0.03 \text{ mm/s}$ . For comparison, the typical difference between a time averaged result and the linear profile for the same rate of strain is  $\delta v_L = 0.14 \text{ mm/s}$ . (The difference between different time averaged profiles is also on the order of  $\delta v = 0.14 \text{ mm/s}$ .) This establishes two things: (1) the ensemble average and time average are measurably different and (2) the ensemble average converges to a linear profile.

These experiments show that athermal fluctuations during flow produce well-defined time-averaged velocity profiles that are not unique. The final state of the system depends strongly on the initial bubble configuration. We expect that this is because the bubble fluctuations during flow do not provide sufficient exploration of phase space to produce time-averaged velocity profiles that are independent of initial conditions. After ensemble averaging, a consistent linear profile emerges, illustrating that time averaging does not equal ensemble averaging for this system. In our experiments this difference is attributed to the athermal nature of fluctuations. In many mesoscopic driven systems, the fluctuations induced by external forcing is co-existent with thermal fluctuations, and the purely athermal effects are difficult to study. In these experiments, we were able to focus on athermal fluctuations because thermal fluctuations are not relevant to the bubble raft. Our results highlight the necessity to distinguish athermal and thermal fluctuations. Future work is necessary to determine the degree to which such differences have a fundamental impact on a statistical mechanics treatment of highly non-equilibrium systems.

This work was supported by a Department of Energy grant DE-FG02-03ED46071. The authors thank Corey O'Hern and Manu for useful discussions.

---

[1] L. Boltzmann, *Wiener Berichte* **63**, 712 (1871).  
[2] L. Boltzmann, *Nature* **51**, 413 (1895).  
[3] L. Boltzmann, *Nature* **52**, 221 (1895).  
[4] L. D. Landau and E. M. Lifshitz, *Statistical Physics (Third Edition), Part 1* (Butterworth-Heinemann, Oxford, 1980).  
[5] R. K. Pathria, *Statistical Mechanics(Second Edition)* (Butterworth-Heinemann, Oxford, 1996).  
[6] L. F. Cugliandolo, J. Kurchan, and L. Peliti, *Phys. Rev. E* **55**, 3898 (1997).  
[7] I. K. Ono, C. S. O'Hern, D. J. Durian, S. A. Langer, A. J. Liu, and S. R. Nagel, *Phys. Rev. Lett.* **89**, 095703 (2002).  
[8] L. Berthier and J.-L. Barrat, *Phys. Rev. Lett.* **89**, 095702 (2002).  
[9] A. J. Liu and S. R. Nagel, *Nature* **396**, 21 (1998).  
[10] F. Zamponi, F. Bonetto, L. F. Cugliandolo, and J. Kurchan, *J. of Stat. Mech. - Theory and Exp.* p. P09013 (2005).  
[11] C. S. O'Hern, A. J. Liu, and S. R. Nagel, *Phys. Rev. Lett.* **93**, 165702 (2004).  
[12] V. Trappe, V. Prasad, L. Cipelletti, P. N. Segre, and D. A. Weitz, *Nature* **411**, 772 (2001).  
[13] C. S. O'Hern, L. E. Silbert, A. J. Liu, and S. R. Nagel, *Phys. Rev. E* **68**, 011306 (2003).  
[14] D. M. Mueth, G. F. Debreygas, G. S. Karczmar, P. J. Eng, S. R. Nagel, and H. M. Jaeger, *Nature* **406**, 385 (2000).  
[15] W. Losert, L. Bocquet, T. C. Lubensky, and J. P. Gollub, *Phys. Rev. Lett.* **85**, 1428 (2000).  
[16] D. Howell, R. P. Behringer, and C. Veje, *Phys. Rev. Lett.* **82**, 5241 (1999).  
[17] P. Coussot, J. S. Raynaud, F. Bertrand, P. Moucheront, J. P. Guilbaud, H. T. Huynh, S. Jarny, and D. Lesueur, *Phys. Rev. Lett.* **88**, 218301 (2002).  
[18] J.-B. Salmon, A. Colin, S. Manneville, and F. Molino, *Phys. Rev. Lett.* **90**, 228303 (2003).  
[19] J. Lauridsen, G. Chanan, and M. Dennin, *Phys. Rev. Lett.* **93**, 018303 (2004).  
[20] P. A. Thompson and G. S. Grest, *Phys. Rev. Lett.* **67**, 1751 (1991).  
[21] S. Y. Liem, D. Brown, and J. H. R. Clarke, *Phys. Rev. A* **45**, 3706 (1992).  
[22] F. Varnik, L. Bocquet, J.-L. Barrat, and L. Berthier, *Phys. Rev. Lett.* **90**, 095702 (2003).  
[23] N. Xu, C. S. O'Hern, and L. Kondic, *Phys. Rev. Lett.* **94**, 016001 (2005).  
[24] N. Xu, C. S. O'Hern, and L. Kondic, *Phys. Rev. E* **72**, 041504 (2005).  
[25] E. R. Nowak, J. B. Knight, E. Ben-Naim, H. M. Jaeger, and S. R. Nagel, *Phys. Rev. E* **57**, 1971 (1998).  
[26] L. Bragg and W. M. Lomer, *Proc. R. Soc. London, Ser. A* **196**, 171 (1949).  
[27] D. Weaire and S. Hutzler, *The Physics of Foams* (Clarendon Press, Oxford, 1999).  
[28] A. Kabla and G. Debrégeas, *Phys. Rev. Lett.* **90**, 258303 (2003).  
[29] D. Weaire, E. Janiaud, and S. Hutzler, *cond-mat* p. 0602021 (2006).  
[30] G. Debrégeas, H. Tabuteau, and J. M. di Meglio, *Phys. Rev. Lett.* **87**, 178305 (2001).  
[31] A. D. Gopal and D. J. Durian, *J. Colloid. Interf. Sci.* **213**, 169 (1999).  
[32] F. Rouyer, S. Cohen-Addad, M. Vignes-Adler, and R. Höhler, *Phys. Rev. E* **67**, 021405 (2003).  
[33] B. Dollet, F. Elias, C. Quilliet, C. Raufaste, M. Aubouy, and F. Graner, *Phys. Rev. E* **71**, 031403 (2005).  
[34] M. Dennin, *Phys. Rev. E* **70**, 041406 (2004).  
[35] Y. Wang, K. Krishan, and M. Dennin, *Phys. Rev. E* **73**,

031401 (2006).